

# DEVELOPMENT OF A REALISTIC PILE-SOIL INTERACTION SYSTEM

by

Salek M. Seraj  
M.S.A. Siddiquee  
M. Shafiqul Bari

*Dept. of Civil Engineering, Bangladesh University of Engineering and Technology, Bangladesh*

## ABSTRACT

In this study an analytical model has been constructed, using the critical state program *CRISP*, and tested against deep (pile) foundations in Dhaka soil. Availability of reliable data of pile load tests performed in- and interaction of piles with both clayey and sandy layers of Dhaka soil prompted a detailed study of various pile-soil systems. A methodology for fixing various mesh parameters has been proposed and the sensitivity of various input parameters of pile-soil system has been studied. The horizontal and vertical extent of soil to be included in the finite element idealization has shown a pronounced effect on the satisfactory prognosis of the system. Although the performance of the finite element model is affected by the thickness of the interface element, for a width-to-breadth ratio of 0.1 for the interface element, such an effect has been found to be minimal. Prior to the final analysis of any pile-soil system, the loading rate has to be determined individually for the case concerned. In case of interaction analysis involving consolidation, it has been observed that excess pore water pressure does not dissipate much during the time span considered in case of pile load testing in the field. The onset of nonlinearity of pile-soil system has been found to be sensitive to the variation of parameters like the unit weight of soil, depth of clay layer, the angle of friction of soil and, of course, the pile size. However, the responses have been found not to be very sensitive to the variation of cohesion, critical void ratio and the slopes of the virgin compression and swelling lines. Although the displacement predictions were affected by the variation in the value of the initial tangent modulus of structural- and soil-elements, the failure load of deep (pile) foundations remained independent of such variations.

## INTRODUCTION

In Dhaka, piles having length 15 m to 20 m are frequently used. The length being quite large, one may encounter three or four different layers of soil having properties varying with depth. A reliable pile load test data (SSE, 1982) was available for Senakallayan Bhaban site at Motijheel, Dhaka. Detailed soil-test report on this site was also available. Thus, the simulation of the model has been conducted for the piles tested in Senakallayan Bhaban site.

For clays, Modified Cam-Clay (MCC) model is used as constitutive law. Sand layers are assumed to follow the elastic perfectly plastic constitutive law. Although, the axially loaded pile essentially represents a three-dimensional problem, since the loading and geometry are symmetrical about the longitudinal axis of the pile, axisymmetric approach permit to reduce it to a two dimensional problem. Accordingly, an axisymmetric analysis has

been performed for axially loaded piles. Pile load tests conducted at Motijheel (SSE, 1982), Kalabagan (IES, 1994) and Green Road (UBE, 1995) have been simulated using conventional laboratory test data. The simulated load-displacement curves match quite well with those of the field pile load test. A more detailed account of the pile-soil system developed here is available elsewhere in Seraj et al., (1997) and Siddiquee et al., (1997).

### MESH CONFIGURATION

Several parameters play important roles for satisfactory performance of any finite element idealizations. Their degree of importance also depends on the objective and type of system on which the analysis is carried out. In this study, seven very crucial parameters are selected (see Fig. 1). The parameters are, the radial extent of mesh from the pile edge ( $C_1$ ); the vertical extent of mesh from pile tip ( $C_2$ ); the rate of change of element size with horizontal distance from pile edge and vertical distance from pile tip ( $m_r$ ), the loading rate ( $L_r$ ); the number of elements along the pile length and its interface with soil ( $N_1$ ); the number of elements within a distance of twice the diameter of pile from pile tip ( $N_2$ ) and the thickness of interface element ( $T_i$ ).

### MATERIAL PROPERTIES

In Bangladesh usually a number of boreholes are dug at a site, both disturbed, and undisturbed samples are then taken for testing in the laboratory. Many parameters show difference in values from borehole to borehole. Consequently, when one has to select single value for all parameters reflecting the nature of the entire site, the task becomes difficult. To avoid this, test results found from boreholes near the testing piles have been given preference and sometimes average of all the related values have been taken in preparing the input data.

In this study, the soil profile has been assumed to consist of two different layers, one is clay and the other is sand below it. Although two different clay and silty-clay layers can be seen, but they are very little different from one another. The sand layer usually extended up to 30 m, which is all the depth that is needed in the present analysis. Altogether six different material types are used in this study. Clay above the water table has been considered to be a separate layer and the clay layer has been set to obey Modified Cam-Clay model while the sand layer is analyzed as elastic-perfectly-plastic model with modulus of elasticity increasing with depth.

#### Clay Parameters

For MCC, the important parameters that are to be assigned are  $\lambda$ ,  $\kappa$ ,  $e_{cs}$ ,  $M$ ,  $\nu$ , and  $G$ . Now,  $\lambda$  and  $\kappa$  parameters can be obtained from oedometer tests or from triaxial tests on samples either isotropically or with  $k_o$ -normally-consolidated (Britto and Gunn, 1987). The frictional constant  $M$  can easily be found from triaxial test (drained or undrained with pore pressure measurement) on isotropically consolidated samples. In the present study, no triaxial test has been conducted and the value of  $\phi'$  for Dhaka clay has been chosen from the data available in Kamal Uddin (1990) and Ameen (1985). The value of  $\phi'$  reported by Kamal Uddin (1990) and Ameen (1985) are  $23^\circ$  and  $25^\circ$ , respectively.

In case of consolidation analysis, co-efficient of permeability values have to be assigned. Here, the permeability in both x and y direction are obtained from the research carried out by Siddique and Safiullah (1995) assuming that  $K_x = 1.5 K_y$ .

### Sand Parameters

The sand layer below the clay layer is analyzed using the elastic-perfectly-plastic model with increasing value of modulus of elasticity with depth. For elastic perfectly plastic material type, the critical parameters that have to be assigned are  $E_0$ ,  $C$ ,  $\phi$ ,  $\gamma_0$  and  $J$ . Here,  $E_0$  is the modulus of elasticity at depth  $y_0$  of soil. This option enables one to assign modulus of elasticity of a certain depth and a corresponding value of the rate of increase of  $E$ . All the values of  $E$  below the specified depth are interpreted by the program using the specified increase rate.

Triaxial tests tend to improve the value of  $E$  since any confining pressure *stiffens* the soil so that a larger initial tangent modulus is obtained. According to Crawford and Burn (1962) *in-situ*  $E$  values generally are 4 to 3 times as large as unconfined compression test value, and 1 to 1.5 times those obtained from triaxial values. Since the laboratory values of  $E$ , although expensive to obtain, do not represent *in-situ* conditions well, SPT and CPT values are widely used to obtain (Stress-strain modulus)  $E$ . Moreover, extensive SPT values at any depth of sand layer of soil can be readily obtained from bore log chart and data as available from standard soil investigation reports. The value of  $E$  can be found by Eq. 1, given by Bowles (1989).

$$E = (15200 \text{ to } 22000) \ln N' \quad (\text{kPa}) \quad (1)$$

If the strain measurement can be done in much finer scale, then the value of initial tangent modulus of stress-strain curves in triaxial test tend to assume a value much greater than what can be obtained from conventional test method. In this respect Iwasaki and Tatsuoka (1977) put forward an equation for calculating  $G$  value using *in-situ* void ratio and  $p'$ . They established empirical equations for shear modulus  $G$  ( $\text{kg/cm}^2$ ) as

$$G = 700 \frac{(2.17 - e)^2}{1 + e} (p')^{0.5} \quad (2)$$

where  $p'$  = mean principal stress =  $(\sigma_1 + 2\sigma_3) / 3$

The value of  $G$  or  $E$  (using  $\nu$ ) obtained from Eq. 2 gives value of  $E$  at least 2 to 3 times larger than the values calculated from Eq. 1. Therefore, the largest value of  $E$  calculated from Eq. 1 can be used in the FE input as it still falls within the conservative range. In this study, usually Eq. 1 has been used to calculate values of  $E$  and sometimes engineering judgement has been applied to arrive representative input values.

Now,  $C$  and  $\phi$  for sand are to be assigned. These values should be obtained from triaxial test results. Although,  $\phi$  values could be evaluated from SPT values using empirical equations, but in this study  $\phi$  value and  $C$  values are obtained from triaxial test results conducted by Yasin (1990). The SPT values tend to predict much larger values of  $\phi$  and are rarely reliable; so the available empirical relations between SPT and  $\phi$  are avoided.

### Interface Parameters

For interface material properties, the parameters that are to be assigned are  $C_a$ ,  $\phi_a$ ,  $K_a$ ,  $G_s$  and  $G_{res}$ . The  $C_a$  and  $\phi_a$  values of interface element should be the  $C$  and  $\phi$  values, respectively, for pile and soil interface; not for soil itself. Thus,  $C_a$  is the adhesion between pile and soil while  $\phi_a$  is the angle of friction between pile and soil. Usually  $\phi_a$  value is slightly lower than  $\phi$  value in case of steel piles but for bored concrete piles, the value of  $\phi_a$  is much higher and can be set to equal to  $\phi$  (Reese et al, 1976). Thus, in this study  $\phi_a$  values are set to be equal to  $\phi$  for respective soil type, i.e., for clay layer  $\phi$  from clay and for sandy layer  $\phi$  from sand have been used.

The modulus in the normal direction of the interface elements ( $K_n$ ) and the shear modulus of interface element ( $G_s$ ) can be calculated from  $E$  and  $\nu$  as follows:

$$K_n = \frac{E(1-\nu)}{(1+\nu)(1-2\nu)} \quad (3) \quad G_s = \frac{E}{2(1+\nu)} \quad (4)$$

If values for  $E$  and  $G$  could be obtained rationally then  $K_n$  and  $G_s$  could also be easily found. The value of  $G_s$  for interface can be obtained from shear test conducted between two dissimilar materials. The residual shear modulus, after the interface element has reached its limiting shear value ( $G_{res}$ ), should have a very low value as it is almost equal to zero in reality. So, in this study,  $G_{res}$  has been assigned to be equal to 10 kN/m<sup>2</sup> arbitrarily to avert the numerical problems, which may take place if such a value is set to zero.

### Pile Material

In this study, the pile is made of reinforced concrete. The pile material has been assumed to be isotropically elastic. It is expected that the main components of displacement at the top of the pile is its elastic shortening. A significant difference in displacement values would occur due to this elastic shortening. Therefore, assigning a representative value of  $E_c$  is very important. The value of  $E_c$  can be obtained from the well known Eq. 5 shown below.

$$E_c = 57500\sqrt{f'_c}, \text{ in psi} \quad (5)$$

If for 3000 psi (20.7 Mpa) concrete,  $E_c$  becomes equal to  $20 \times 10^6$  kPa. But it is well known that by confining a concrete in two out of three mutually perpendicular directions, the ultimate compressive strength of the element in the third direction increases considerably and in practice, confinement is usually passive, and provided by steel, which, due to the elongation imposed on it by the lateral expansion of concrete, induces compressive stresses in the element (Kinoshita et al., 1994). As the pile being analyzed has been constructed using spiral tie bars which is an effective form of passive confinement, the value of  $E_c$  is expected to be considerably higher than Eq. 5 estimation. In light of this understanding, the value of  $E_c$  has been used, although still underestimated, as  $30 \times 10^6$  kPa for 20.7 MPa concrete. Tables 1, 2, 3 and 4 represent all the material properties used for pile A, pile B and Pile C in this model in the light of previous discussions.

### In-Situ Stresses

The satisfactory performance of the FE model depends heavily on the accurate use of *in-situ* stresses, which vary from point to point in the soil. The *in-situ* stresses that are to be assigned in the present model are  $\sigma'_v$ ,  $\sigma'_h$ ,  $U_o$  and  $p'_c$  for the entire region of the mesh. To determine these *in-situ* stresses, an empirical method based on the data accumulated by Wroth (1975) has been used in this study. *In-situ* stresses can be specified in every integration point for each element and it could also be specified for certain horizontal layers when *in-situ* stresses for each element is interpolated from the given set of reference points representing layers. In this study, the second option has been used as this is much easier to specify and is accurate as well. The detailed *in-situ* stresses for pile A are shown in Table 5.

### Description of Piles

#### Pile A

Pile A had a diameter of 0.508 m and it was 19.3 m long. The soil profile at the location of pile A is characterized into distinct layers as clay and sands below the clay layer, based on the SPT value and available soil test report. Figure 2 shows these layers along with SPT values at various depth.

### Pile B

The site concerned is at Kalabagan, Dhaka (IES, 1994) and the present pile would be designated as Pile B throughout the text. Soil exploration i.e. bore log chart with gradation curve, unconfined compression test and  $(\log_{10} \sigma_v, e)$  curve and of course, the pile load-test data were available for Pile B. Pile B is of 15.25 m height and 0.458 m diameter. The various material parameters needed as input to the FE model are available in Tables 1, 2, 3, 4, 5, and Fig. 3.

### Pile C

The third pile is a bored pile cast at Green road, Dhaka (UBE, 1995) and designated as Pile C in this study. Pile C is only 11m in length and 0.432 m in diameter. The necessary values of all parameters including material properties and mesh configuration properties are given in Tables 1, 2, 3, 4, 5 and in Fig. 4

### FINITE ELEMENT DETAILS

In this study, 8-noded linear strain quadrilateral element with displacements unknown (Fig. 5) has been used for both pile elements and soil elements in case of drained or undrained analysis. But for consolidation analysis, soil elements under water table have been selected to be linear strain quadrilateral with displacement and excess pore pressures unknown (Fig. 5). For interface elements, the 6 noded interface element with displacement unknown is used. All these elements are basically standard displacement finite elements (Zienkiewicz, 1977). The positioning of interface elements along pile shaft specially near the tip calls for a special treatment. All along the pile shaft, the interface elements are rectangular having the longer dimension along the pile. But at the tip of pile the interface elements are set to be trapezoidal as shown in Fig. 5. This has been done to avoid the placement of one vertex of interface element on the side of the soil element below which no node is present. If a node is placed at that point, then the aspect ratio of all soil elements below would have been too large for accurate analysis.

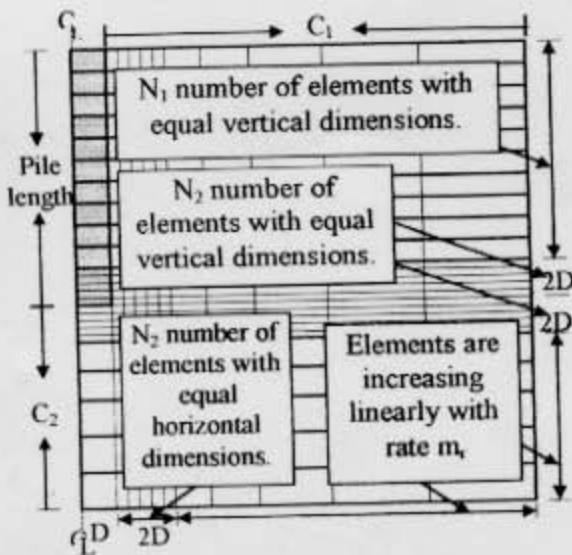


Fig. 1 Various critical mesh parameters

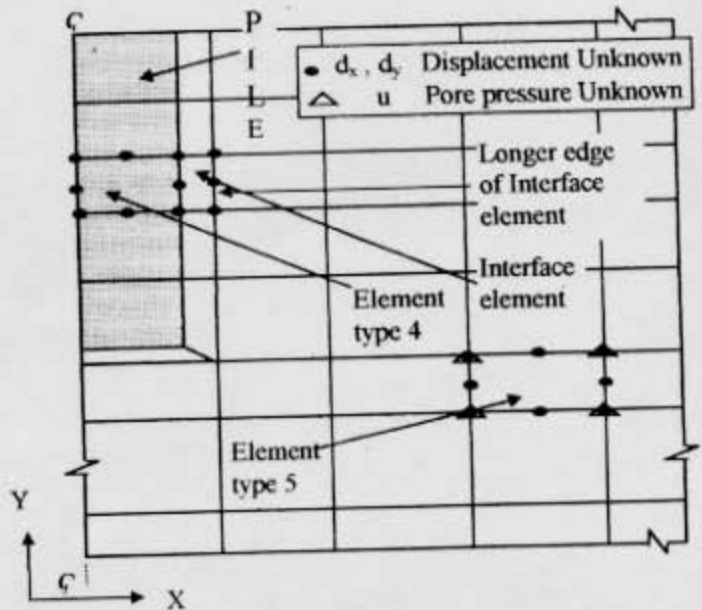


Fig. 5 Different types of elements used in this study.

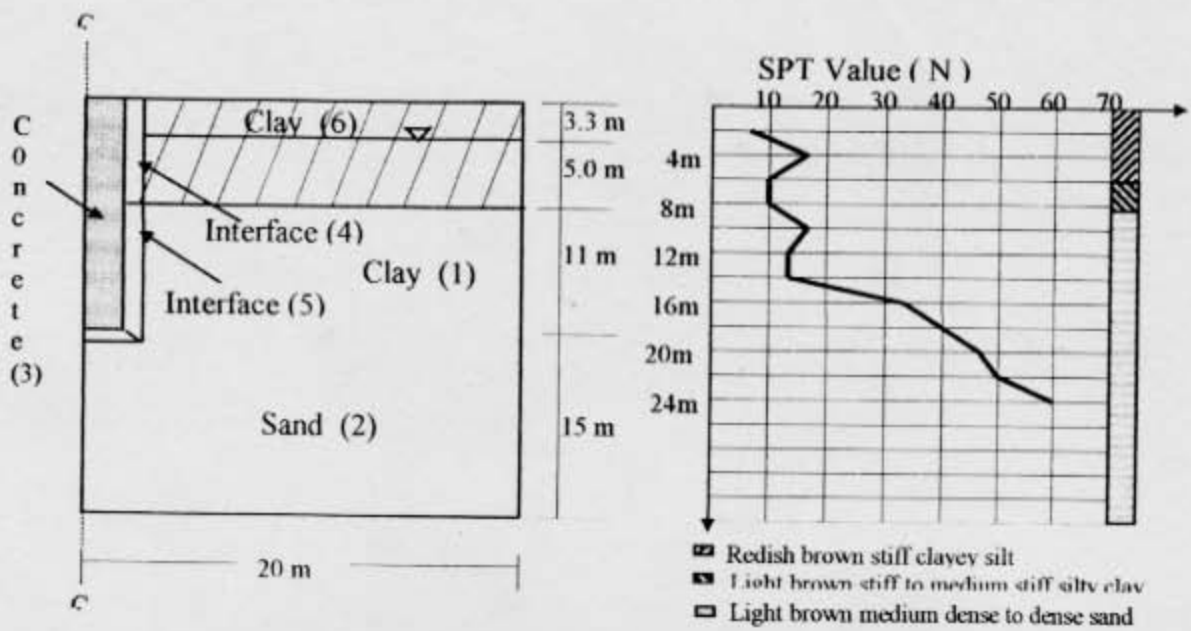


Fig. 2 The soil profile along with SPT values for Pile A

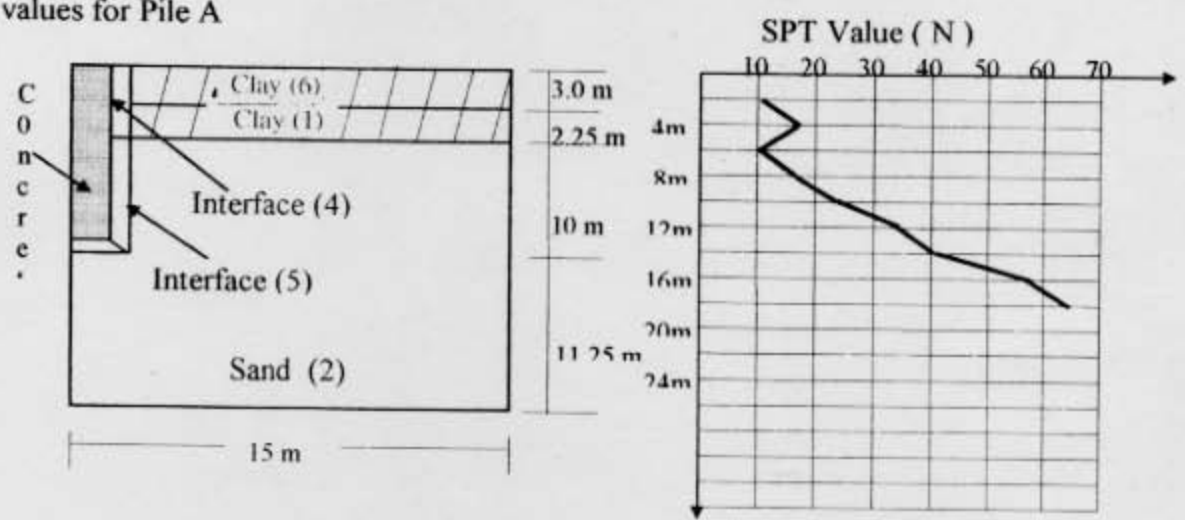


Fig. 3 The soil profile along with SPT values for Pile B

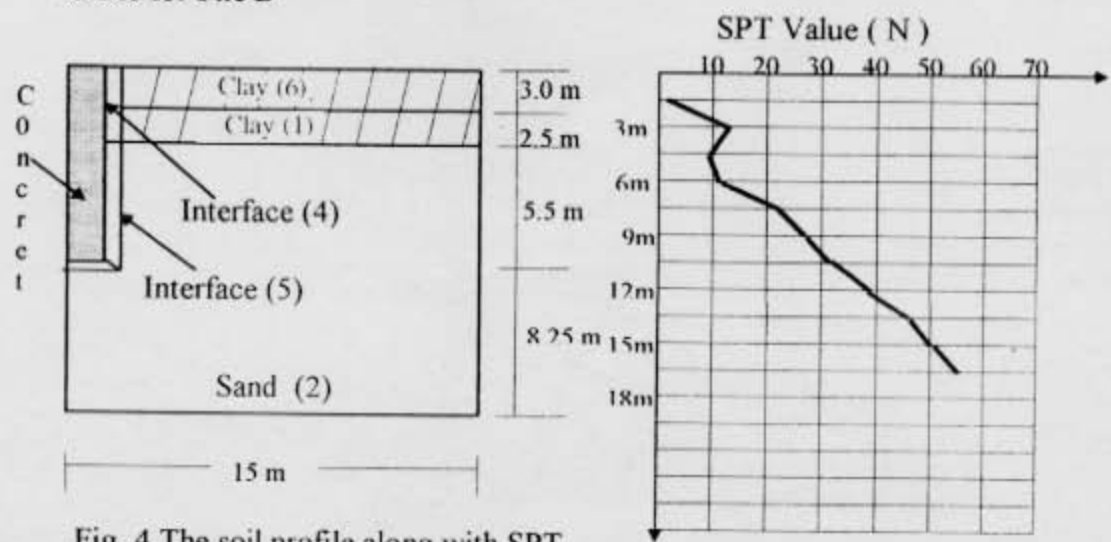


Fig. 4 The soil profile along with SPT values for Pile C

## OPTIMIZATION OF MESH CONFIGURATION

Several parameters play important roles for satisfactory performance of any finite element idealizations. In this study, seven very crucial parameters were optimized and a mesh was created (Fig. 1). The parameters were, the radial extent of mesh from the pile edge ( $C_1$ ); the vertical extent of mesh from pile tip ( $C_2$ ); the rate of change of element size with horizontal distance from pile edge and vertical distance from pile tip ( $m_r$ ), the loading rate ( $L_i$ ); the number of elements along the pile length and its interface with soil ( $N_1$ ); the number of elements within a distance of twice the diameter of pile from pile tip ( $N_2$ ) and the thickness of interface element ( $T_i$ ).

### Determination of $C_1$

Firstly, the effect of variation of  $C_1$  in the load-displacement curve is investigated which is shown in Fig. 6. It shows that for all values of  $C_1$  other than for  $C_1$  equal to 5 m and 10 m, the load-displacement curves have very insignificant or no difference. For  $C_1$  equal to 10 m, the curve deviates from the others slightly and for  $C_1$  equal to 5 m, the curve deviates considerably from the convergent group. Therefore, as far as load-displacement behaviour is concerned, a value of 15 m for  $C_1$  may be considered to be an acceptable value for predictions without impairing accuracy.

In order to substantiate the above finding, a new parameter of stress, which represents the overall stress conditions of any element, has been introduced. This is called the Stress-norm ( $\sigma_{sn}$ ) which can be calculated as follows:

$$(\sigma_{sn})_i = \left| \sqrt{(\sigma_x)^2 + (\sigma_y)^2 + (\sigma_z)^2 + (\tau_{xy})^2} \right| \quad (6)$$

Where,

$(\sigma_{sn})_i$  = stress-norm of element  $i$ ,  $\sigma_x$  = normal stress of element  $i$  in  $x$  direction caused by extra load on pile top only,  $\sigma_y$  = normal stress of element  $i$  in  $y$  direction caused by extra load on pile top only,  $\sigma_z$  = normal stress of element  $i$  in  $z$  direction caused by extra load on pile top only and  $\tau_{xy}$  = shear stress of element  $i$  in  $xy$  plane caused by extra load on pile top only.

It can be seen from Fig. 7 that  $\sum(\sigma_{sn})_i$  for all elements along  $BD_1$  decreases with increasing values of  $C_1$ . It is also clear that for all values of  $m_r$  analyzed, the trend is similar and all curves converge as  $C_1$  takes larger values. Starting from a value as high as more than  $10 \text{ kN./m}^2$ ,  $\sum(\sigma_{sn})_i$  reaches a value as low as below  $0.4 \text{ kN/m}^2$ . For  $C_1$  ranging from 5 to 15 m, the value of  $\sum(\sigma_{sn})_i$  decreases sharply, but after that decreases very slowly with increasing  $C_1$ . Therefore, the convergence of load-displacement curves for  $C_1$  equal to 15 m or greater (Fig. 6) is justified as the values of  $\sum(\sigma_{sn})_i$  for them are very insignificant.

Conservatively, the value of  $C_1$  has been selected to be 20 m. In this case the value of  $C_1$  equals to the length of pile ( $H$ ). In the subsequent analysis,  $C_1$  has been taken to be equal to  $H$ ; the ensuing findings as well as cross-checks proved that the use of  $C_1$  equal to  $H$  is justifiable in all respect.

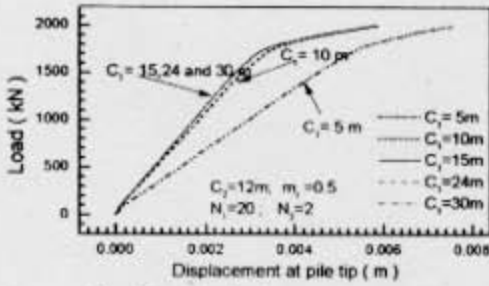


Fig. 6 Load-displacement curves for various radial extent of mesh.

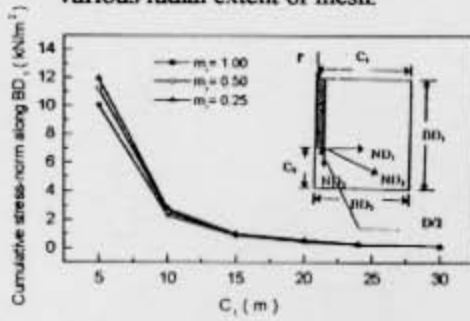


Fig. 7 Variation of cumulative stress-norm along boundary  $BD_1$  with radial distance.

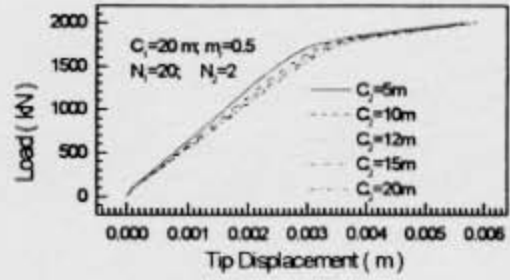


Fig. 8 Load-displacement curves for various depths of mesh below pile tip.

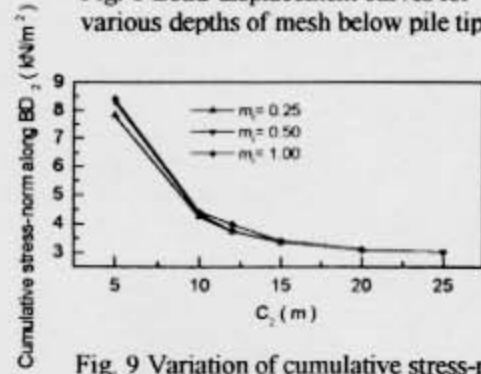


Fig. 9 Variation of cumulative stress-norm along  $BD_2$  with radial distance from pile.

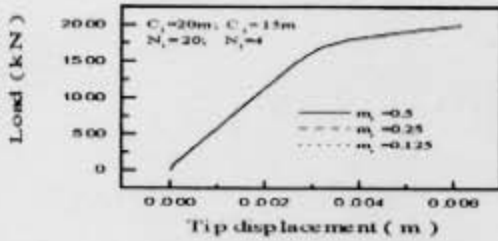


Fig. 10 Load-displacement curves for various  $m_1$ .

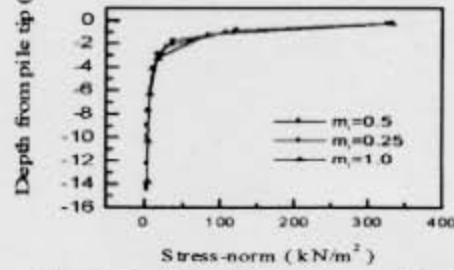


Fig. 11 Variation of stress-norm with depth from pile tip.

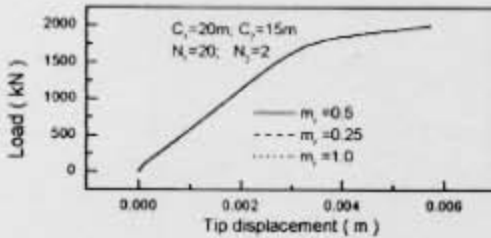


Fig. 12 Load-displacement curves for various  $m_1$ .

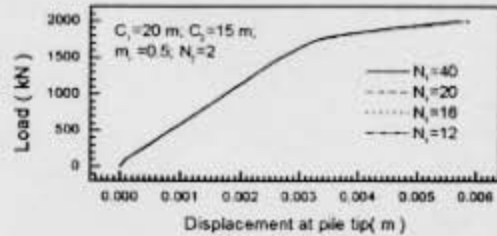


Fig. 13 Load-displacement curves for various  $N_1$ .

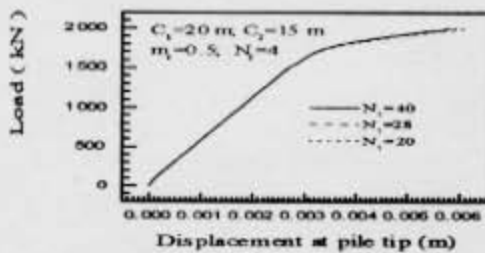


Fig. 14 Load-displacement curves for various  $N_1$  (when  $N_2=4$ ).

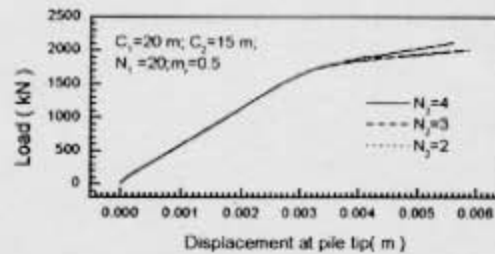


Fig. 15 Load-displacement curves for various  $N_2$ .

### Determination of $C_2$

The effect of variation of  $C_2$  on the load-displacement curve of pile is shown in Fig. 8. The figure shows that for increasing values of  $C_2$ , the curves tend to shift rightwards slightly. At the region, where transition from linear state to nonlinear state occurs, the rightward shifts are most significant. After that region, curves start converging. From engineering point of view, the values of  $C_2$  equal to 15 m, 20 m or 25 m are equally good as they represent very little difference in the load at the onset of significant nonlinearity. It can be expected that for very large values of  $C_2$ , the load-displacement curves would converge completely. But increase in the running time cost, would make the use of a very large value of  $C_2$  less attractive as reasonable results could easily be obtained by using a smaller value of  $C_2$ .

Fig. 9 shows the variation of  $\sum(\sigma_{sn})_i$  for boundary 2 i.e.  $BD_2$  with increasing value of  $C_2$ . As expected, the values of  $\sum(\sigma_{sn})_i$  decreases exponentially with increasing value of  $C_2$ . For values  $C_2$  between 5 to 15 m, the curves show significant decline, but after that the rate of decrease becomes sluggish and use of a very large value of  $C_2$  (say  $C_2$  equal to 30 m) would result in very little improvement in the load deflection behavior. It should be noted here that the value of  $\sum(\sigma_{sn})_i$  in the present case did not converge to an insignificant quantity as was the case with  $C_1$ .

It may be concluded, admittedly tentatively, that the use of  $C_2$  equal to  $3/4 H$  (i.e. 15 m in the present case) may lead to satisfactory prognosis in all cases with  $m_r$  equal to 0.5 or less. This has been substantiated elsewhere in Seraj et al. (1997).

### Determination of $m_r$

Till now, three different values for rate of increase of element dimension have been investigated for fixing  $C_1$  and  $C_2$ . This article deals exclusively with the effect of  $m_r$  on the predicted response and a fourth value of  $m_r$  has also been investigated here for better and confident understanding of the problem. Other parameters have been fixed in the light of previous sections and they are presented in Table 6

Figure 10 shows the effect of varying  $m_r$  on load-displacement curves. It is clear from Fig. 10 that for the three values of  $m_r$  used in this analysis, the load-displacement curves completely converge into one. Therefore, there is no practical benefit in using much finer mesh than the meshes adopted in this study. However, since the use of  $m_r$  equal to 1.0 results in too high value of aspect ratio for some elements distant from pile, for satisfactory finite element analysis a value of  $m_r$  equal to 0.5 appears to be reasonable.

Figures 11 and 12 show that the effect of increasing dimensions of elements is more pronounced within say 5 m of pile tip and beyond that point, higher rate of increase of mesh size can be adopted. Therefore, it appears to be a better approach to select smaller increase rate for first 5 m or ( $H/4$  in the present case) distance from pile and a larger increase rate for elements beyond that region.

In this analysis, the number of elements within a distance of  $2D$  from pile tip ( $N_2$ ) has been taken to equal to 2. If finer mesh is adopted in that region (say  $N_2$  equal to 4), the effect of  $m_r$  on load-displacement curves may slightly differ from those shown in Fig. 10. Here, the value of  $N_2$  may be selected as 4 in some of the analyses. The effect of varying  $m_r$  for the case of  $N_2$  equal to 4 is worth investigating. Figure 12 show the load-displacement curves for

varying  $m_r$  in case of  $N_2$  equal to 4. Once again these curves converge into one curve pointing out that the selection of  $m_r$  equal to 0.5 is satisfactory. Here, even a smaller value of  $m_r$  ( $= 0.125$ ) has been investigated with others. It is clear that this value of  $m_r$  does not improve the practical aspect of the analysis at all.

This nonchalance of load deflection behavior with variation of  $m_r$  is quite expected as the dimension of element along interface is unchanged and a finer mesh is used in the region within  $2D$  of pile tip. The variation of  $m_r$  is not sensitive enough as long as the aspect ratio be within reasonable limits. After all these analysis, the value of  $m_r$  has been selected to be 0.5 or equal (the diameter,  $D$ ) of the pile.

#### **Determination of $N_1$**

The size of elements connecting interface elements should be equal as otherwise, it would be difficult, in the present case, to keep the aspect ratio of interface elements within specified limit (Desai et al, 1984). In this analysis, it has been tried to keep the size of elements adjacent to interface elements constant and subsequently, vertical dimension of all elements within the soil surface and pile tip have been kept constant. Here  $N_1$  is the number of these equal length elements along the pile length.

The effect of the variation of  $N_1$  on load-displacement behavior is investigated and shown in Fig. 13. It can be seen from Fig. 13 that the increase of the number of elements along pile shaft over 20 does not produce any benefit as both the curves for  $N_1$  equal to 20 and 40 almost converge to one. Other lower values of  $N_1$  such as  $N_1$  equal to 16 or 12, produce gradual deviation from the converged group, as expected. But these deviations are small enough to be of any tangible significance.

It can be stated that the use of the value of  $N_1$  equal to 20 is adequate for all practical purposes as increased number does not bring any difference. However, if the number of elements in the region within twice the diameter of pile tip ( $N_2$ ) is increased as it would be the case in the next section, then the selection of  $N_1$  may have to be reviewed giving due consideration to aspect ratio. Keeping this view in mind, a study has been done with a increased value of  $N_2$ . For this increased value of  $N_2$  ( $N_2=4$ ), the effect of increase in the value of  $N_1$  on the load-displacement response has been shown in Fig. 14. This figure shows that, with increased  $N_2$ , the load-displacement curves for increasing value of  $N_1$  produce some deviation from each other and they do not form a single line as was the case for  $N_2$  equal to 2. But once again, the deviations or improvements in the value of  $N_1$  above 20 are insignificant from practical point of view. As the increase in the value of  $N_1$  increases the running time, such an increase is not obligatory. From all these extensive analyses, it can be concluded that the value of  $N_1$  may be set at 20 (i.e.  $H/2D$  as put in the present case).

#### **Determination of $N_2$**

Much importance should be given to the dimension of elements near the pile tip as this is the highly stressed zone of a pile. The radial extent of this high stress zone, for which element dimensions should be smaller, has been fixed at twice the diameter of the pile ( $2D$ ) in any direction from pile tip as shown in Fig. 1. The role of the number of elements (or the size of elements) in this zone have been investigated in this section. The other parameters used here are presented in Table 7 along with different values of  $N_2$ .

Figure 15 shows the effect of varying  $N_2$  on load-displacement behavior. It can be seen from the plot that an increase in the value of  $N_2$  predicts more deflections, as expected. But the plots do tend to come together for greater values of  $N_2$ . In order to investigate whether the high-stressed zone with denser mesh should be extended below the pile tip beyond  $2D$ , a study was undertaken by Seraj et al. (1997) which revealed that the use of  $N_2$  equal to 4, i.e. the size of elements in high-stressed zone equal to  $D/2$  is acceptable.

#### **Determination of $T_i$**

The selection of thickness of interface element,  $T_i$ , is just as important as selecting the soil parameters in any soil-structure interaction problem. For the small thickness interface element proposed by Desai et al (1984) which has been incorporated in this study, the dimension of interface elements should be such that  $T_i/b$  ratio remains within 0.1 to 0.01.

The effect of varying interface element thickness on the load-displacement behavior has been shown in Fig. 16. This load-displacement plot shows that a great deal of deviation of behavior occurs for  $T_i$  equal to 0.025 and 0.0125 with respect to  $T_i$  equal to 0.05. However, the curves for the value of  $T_i$  equal to 0.025 and 0.0125 almost come together.

Therefore, it can be concluded that the use of interface thickness keeping  $(T_i/b)$  ratio within specified limit is good enough while other values not abiding by this constraint should be avoided. But as long as the  $(T_i/b)$  ratio is within 0.1 to 0.01, there is no need to go for much fineness than necessary as these would not make much difference to the analysis. Thus, the thickness of interface element may be selected at 0.025 m (which is equal to one tenth of the dimension of adjacent smallest elements). Accordingly, the value of  $T_i$  in this study has been fixed at  $1/10(D/2)$  i.e.  $D/20$ .

### **PILE LOAD TEST SIMULATION**

After the material parameters and optimum mesh configuration have been fixed, as shown in Table 8, a consolidation analysis with the same time increment as used in the load test has been performed for pile A, B and C. Loading increment and size of interface elements also have been obtained from those parametric studies. When all the geometry and element parameters along with material properties have been selected rationally, then the final model has been put to final run. This section deals with a thorough comparison of the actual pile load test with response obtained from its numerical simulation.

#### **Load-Displacement Response**

The predicted load-displacement response obtained from the FE analysis using consolidation is presented in Fig. 17, Fig. 18 and Fig. 19 along with load displacement curve obtained from pile load-tests conducted on pile A, B and C. It shows that the predicted load displacement curve resembles the load-test curve reasonably. Although the actual load-test curves show slightly less displacement than its numerical counterpart, this prediction could be considered as an acceptable prediction from the engineering point of view. This higher FE displacement prediction is, however, quite natural and expected keeping in mind that various material properties selected actually were on the somewhat conservative side. Accordingly, the prediction is on the safer side.

Looking carefully into the causes for this extra displacement, one can easily find that some critical parameters that were assigned had conservative values. Firstly, the actual initial tangent of the stress-strain plot giving the modulus of elasticity of soil is much greater than the value found from traditional triaxial testing. Here the angle of internal friction of soil has

also been selected conservatively. The actual soil profile consists of many layers. In the present study, the adopted soil profile has been simplified to have only two layers, the clay layer with uniform properties and the sand layer with increasing  $E$  with depth. Whereas the Dhaka soil is actually preconsolidated, the presently adopted assumption of normally consolidated behavior invariably predicted less *in-situ* stresses, which may result in substantial increase in displacements. Above all, there are several parameters that are to be determined from laboratory testing at almost every meter of depth of soil for at least for 35 m depth, in order to faithfully prepare input data so that closer prediction of the actual pile load test could be achieved. However, for all practical purposes and after considering the variability of various parameters as well as cost involved, it is neither warranted nor possible to have an all encompassing match between physical and numerical tests.

It can be further noted here that the actual *in-situ* pore-water distribution for the whole soil depth concerned has to be found out and used for accurate prediction of consolidation settlement. Presently, the *in-situ* pore pressure has been assumed to be the same as static head distribution, i.e. linear increase of pore-pressure from water table. But actual pore pressure distribution may be quite different from the assumed profile. This has certainly affected the prediction.

In view of all these it can be stated that the presently demonstrated numerical prediction matches the real response reasonably well. The displacements predicted may be slightly higher, but the failure load, the load at which considerable non-linear displacement occurs, seems to match the actual value well. The overall trend of both curves are similar too.

The elastic shortening of pile itself is a considerable part of the total displacement at the top of the pile. If the Figure 17 which shows the load displacement curve at the pile tip is looked at, it becomes clear that the difference between displacement at pile tip and pile top for a particular load is considerable and is equal to the elastic shortening of the pile material. Here, Pile A is a concrete pile with closely space spiral confinement. It has been found (Kinoshita et al., 1994) that the strength of concrete (also the elastic modulus) increases significantly when subjected to confinement, both active and passive. It can increase even up to 4 to 5 times than the values of uniaxial compressive strength of concrete. Hence, the pile used in this study has much greater  $E_c$  value than the value used, due to possible confinement of concrete and this would certainly account for much of the differences in displacement observed in Fig. 17. Had the value of  $E_c$  been increased, the curve of displacement at pile top would have moved leftwise and better correlation with the pile load test would have been obtained.

### **Pile Load Transfer**

The predicted load transfer characteristics for pile A is shown in Fig. 20(a). Also, the propagation of slippage for different loads have been shown in Fig. 20(b). Figure 20(a) shows that the load transfer in sand layer is much higher than clay layer, as expected. Almost all the loads are transferred to the soil by interface shear and a very small portion of the applied load is resisted by the pile tip. This signifies that a major portion of pile load is transferred through frictional resistance. Thus, the condition in which both frictional resistance and tip bearing resistance would be attained has not reached in the case studied.

Figure 20(b) depicts the slippage zone and its propagation with increasing load. First slippage occurs after more than 1100 kN of load and it starts in the beginning of the sand layer rather than the clay layer. With increasing load, the slippage moves both upward and

downward upto 2030 kN load when almost all other zones show slippage. There is also some slippage near the pile tip. One thing should be noticed here that the initial clay layers which is above the water table has not slipped at all, as the effective *in-situ* stress is relatively greater here than the clay layer below the water table. So, the shear stresses developed in the interface of this layer have not reached its capacity.

The reason for starting of slippage first in the sand layer rather than in clay layer lies in the interface shear resisting properties of the two layers. In clay layer there is adhesion ( $C_a$ ) with friction ( $\phi$ ) which resist shear, but in sand layer only frictional shear resistance comes into action. As a result, the shear capacity in the interface between pile and sand layer starts to reach limiting state first.

The interface element is formulated in such a way that it controls the slippage and the load transfer. Figure 21(a) shows the shear stress distribution of interface elements along the pile shaft. It is observed that the shear-stress in interface elements start to reach limiting value first at 1120 kN of load as was shown in Fig. 20(b) too. With increasing load, these shear stresses reach limiting values gradually along the shaft depth of pile in sand layer. When 1540 kN load is applied, the shear stress of the whole depth seem to reach limit and after that load, the shear stresses do not increase considerably.

If the shear stress distribution of soil elements adjacent to interfaces is looked at in Fig. 21(b), it is clear that these soil elements have shear stresses varying in the same manner as in the interface elements. When the shear stresses in interface reaches their limiting state, the shear stresses in adjacent soil elements does not increase any more.

The shear stress contours for 560 kN, 1560 kN and 2030 kN are shown in Figures. 22(a), (b) and (c), respectively. All these plots show that the maximum shear stresses develop near the shaft of pile with a tendency of shear stress concentration near the pile tip. As the pile transfers load predominantly as friction along the shaft, this pattern of shear stress contours is quite expected. When the tip resistance would be significant, only then maximum shear would occur below the pile tip. Besides, the contours seem to become uniformly varying in the sand layer as sand layer has greater shear strength.

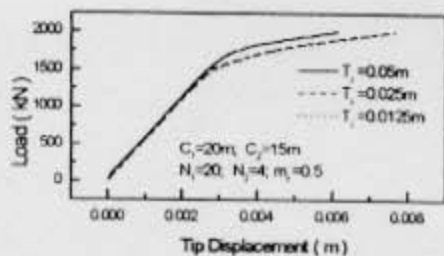


Fig. 16 Load-displacement curves for various  $T_i$ .

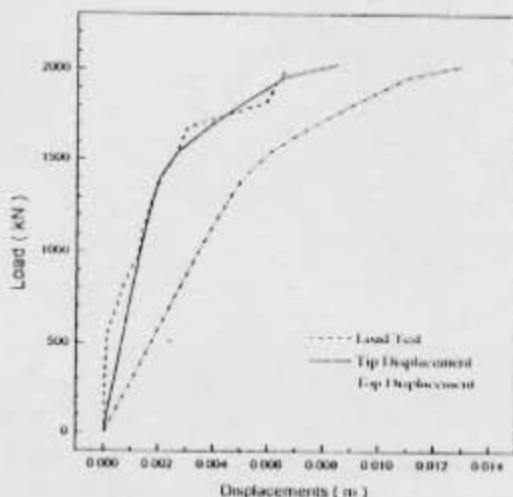


Fig. 17 Load-displacement curves for Pile A

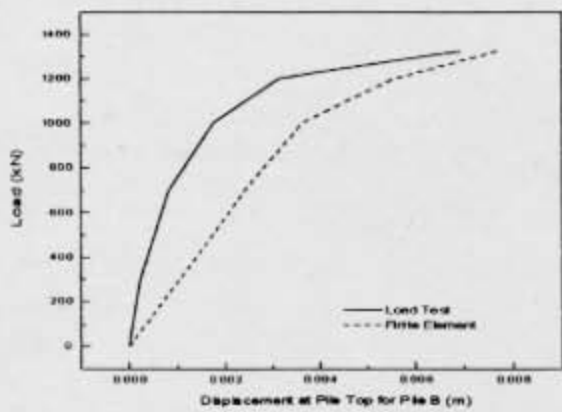


Fig. 18 Load-displacement curves for Pile B

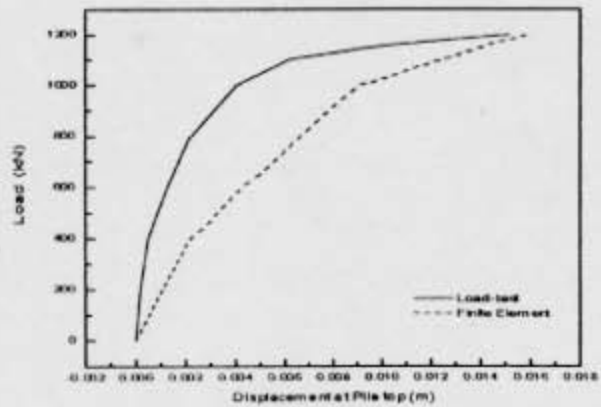


Fig. 19 Load-displacement curves for Pile C

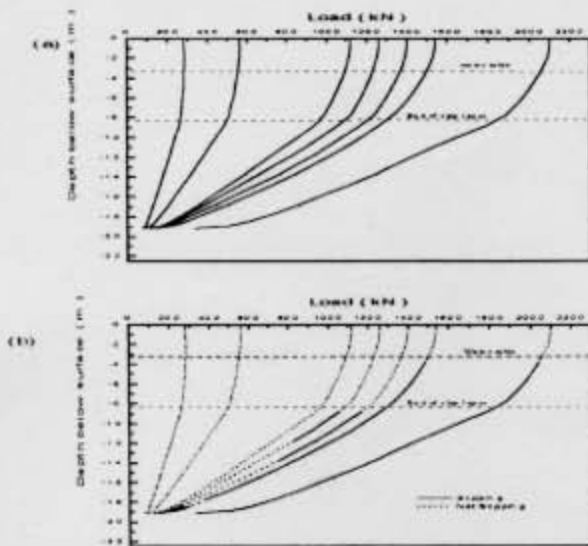


Fig. 20 (a) Pile load transfer (b) slippage propagation

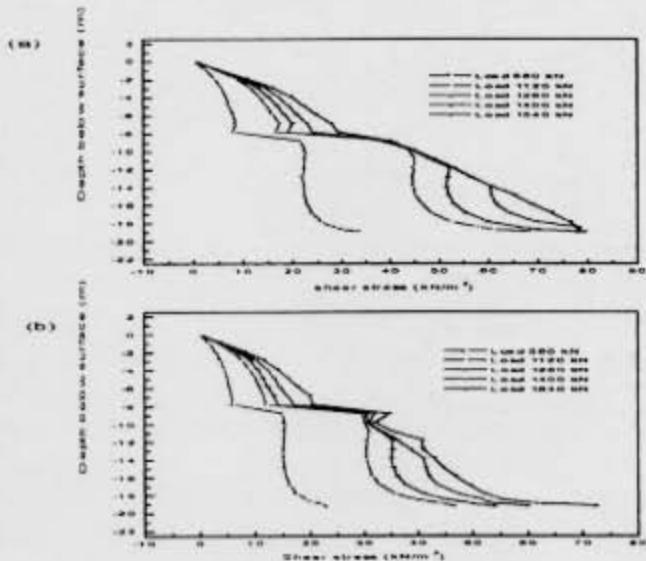


Fig. 21 Shear stress distribution (a) Interface (b) Adjacent to interface

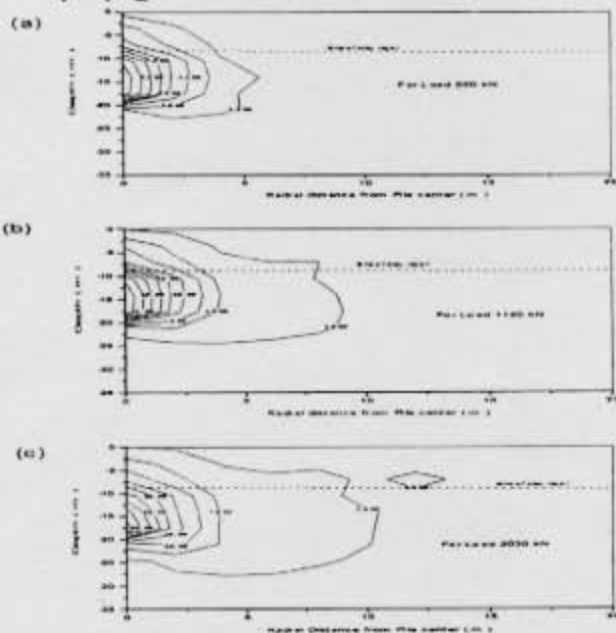


Fig. 22 Shear stress contour at different stress

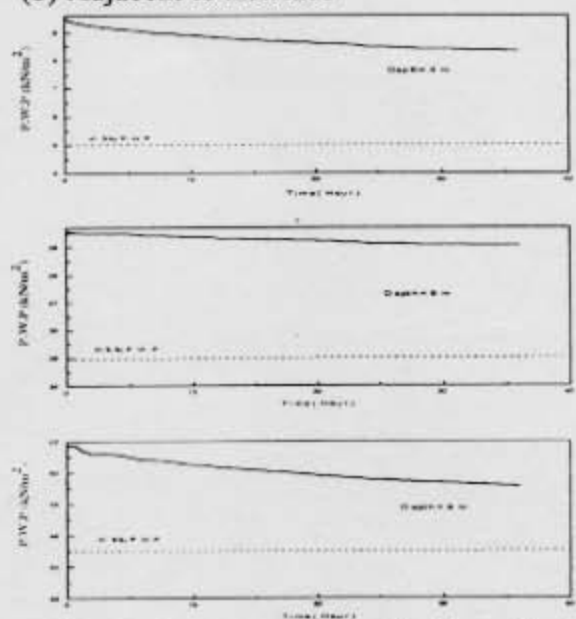


Fig. 23 Pore pressure distribution with time.

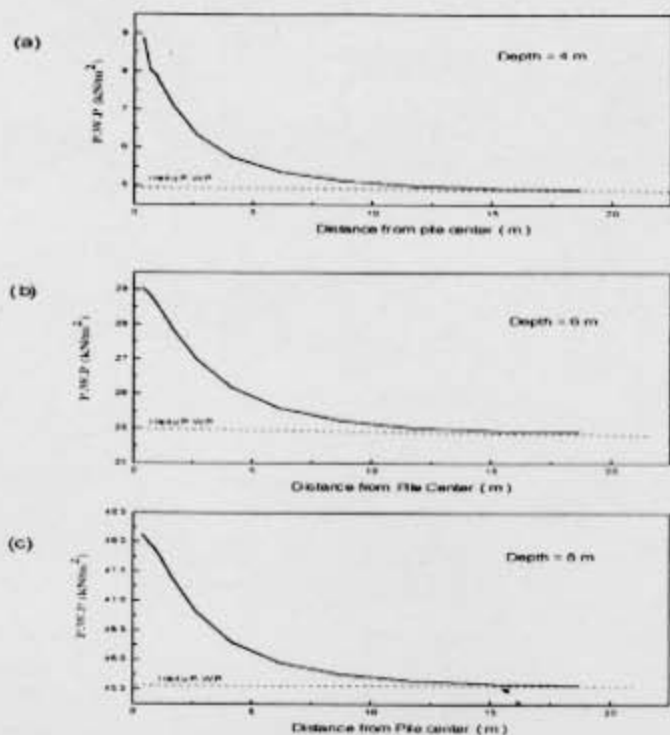


Fig. 24 Pore pressure distribution with radial distance from pile centre for (a) 4m, (b) 6m and (c) 8m depth.

distance from pile shaft center for all three depths discussed earlier. These figures indicate that where as significant pore pressure develops near the pile shaft, some distance away from it, the pore water pressures assume in-situ value again. This confirms that the consolidation settlements are concentrated only close to the pile and it is insignificant some distance away from the pile.

### CONCLUSIONS

The following conclusions may be drawn from the present study.

1. The horizontal and vertical extent of soil to be included in the finite element idealization has a pronounced effect on the predicted response of the system. In this study specific non-dimensional guidelines have been suggested and subsequently tested for obtaining reasonable mesh configurations. The proposed methodology may be suitably adopted to other structure-soil systems.
2. Satisfactory performance of the finite element model is affected by the thickness of the interface element. It has been found that for a width-to-breadth ratio ( $t/b$ ) of 0.1 for the interface element, effect is minimal.
3. Prior to the final analysis of the pile-soil system, the loading rate has to be determined individually for the case concerned. The methodology suggested in this study may be adopted for such a selection.
4. Realistic material parameters of soil and structural elements are very important for the model to simulate any pile-soil system properly. Special care should be taken in

### Pore Water Pressure

The excess pore water pressure developed and their dissipation with time for different depth in clay layer are shown in Figures. 23(a), (b) and (c). For the time span shown, as used in pile load test, it is evident that very insignificant excess pore pressure has been dissipated. Hence, the subsequent displacement due to consolidation is very nominal as compared to the immediate displacement, which is also the case in actual load test. For the three depth selected in these plots, 4 m and 8 m depth show more excess pore pressure dissipation than for 6 m depth. This is so because the other two depths are near the drained boundaries. But depth of 6 m is deep in the clay layer, so it is taking much greater time than the other two to dissipate the excess pore pressure.

Figures 24(a), (b) and (c) show the dissipation of pore pressure with radial

specifying *in-situ* stresses in soil prior to the installation of the structural member in order to simulate real field behavior.

5. While studying the interaction of pile-soil system, it has been revealed that the horizontal and vertical extent of soil to be included in the finite element idealization has a pronounced effect on the predicted response of the system. The proposed methodology may be suitably adopted to other structure-soil systems.
6. Prior to the final analysis of the soil-structure system, the loading rate has to be determined individually for the case concerned. The methodology suggested in this study may be adopted for such a selection.
7. In case of consolidation analysis, it was observed that the excess pore water pressure did not dissipate much for the time span considered in case of pile load-testing in the field. Besides, the excess pore water pressure development has found to occur mainly near the pile. The pore pressure assumes the *in-situ* value at some distance away from it.
8. The onset of nonlinearity of concrete pile -soil system has been found to be sensitive to the variation of parameters like the unit weight of soil, depth of clay layer, the angle of friction of soil and, of course, the pile size. On the other hand, the responses have been found not to be very sensitive to the variation of cohesion, critical void ratio and the slopes of the virgin compression and swelling lines. Although the displacement predictions were affected by the variation in the value of the initial tangent modulus of structural and soil elements, the failure load of deep (pile) foundations remained independent of such variations.

#### REFERENCES

- Britto, A.M. and Gunn, M.J. (1987), *Critical State Soil Mechanics Via. Finite Elements*, John Wiley & Sons Limited, New York.
- Ameen, F. (1985), "Geotechnical Characteristics of Dhaka Clay", M.Sc. Engg. Thesis, Department of Civil Engineering, Bangladesh University of Engineering and Technology, Dhaka.
- Bowles, J.E. (1989), *Foundation Analysis and Design*, McGraw-Hill International Book Company, Fourth Edition, New York.
- Britto, A.M. and Gunn, M.J. (1987), *Critical State Soil Mechanics Via. Finite Elements*, John Wiley & Sons Limited, New York.
- Crawford, C.B. and Burn, K.N. (1962), "Settlement Studies on the Mt. Sinai Hospital", *Engineering Journal of Canada*, Ottawa, vol. 45, No. 12, December.
- Desai, C.S., Zaman M.M., Lightner, J.G. and Siriwardane, H.J. (1984), "Thin-layer Elements for Interfaces and Joints", *Int. Jnl. for Numerical and Analytical Methods in Geomechanics*, V.8, 19-43.

Icon Engineering Services (IES), (1994), H-79/F Airport Road, Banani, Dhaka, "Report on-Geotechnical Investigation for Construction of Multistoried Building", Property Pair at Kalabagan, Dhaka.

Iwasaki, T. and Tatsuoka, F. (1977), "Effects of grain size and grading on dynamic shear moduli of sands", *Soils and Foundations*, Vol. 17, No. 3, pp. 19-35.

Kamal Uddin, M. (1990), "Compressibility and Shear Strength of Remoulded Dhaka Clay", M.Sc. Engg. Thesis, Department of Civil Engineering, Bangladesh University of Engineering and Technology, Dhaka.

Kinoshita, M., Kotsovos, M.D. and Pavlovic, M.N. (1994), "Behavior of Concrete under Passive Confinement", Proc. JSCE, J. Materials. Conc. Struct. Pavements, No. 502, vol. 25; 131-142.

Reese, L. C., Touma, F.T. and O'Neill, M.W. (1976), "Behavior of Drilled Piers under Axial Loading", *Int. Geot. Eng. Div., ASCE*, vol. 102, GT5;493-510.

Seraj, S. M., Siddiquee, M. S. A. and Bari, M. S. (1997), "Development of a Methodology for determining Optimum Mesh Configuration", submitted to IJNME for publication.

Siddique, A. and Safiullah, A.M.M. (1995), "Permeability Characteristics of Dhaka Clay", *Journal of the Civil Engineering Division, IEB*, vol.23/CE, no.1.

Siddiquee, M. S. A., Seraj, S. M. and Bari, M. S. (1997), "Realistic Simulation of Pile Load Test", Submitted for Publication.

Subsoil Engineers (SSE), (1982), 39 New Elephant Road, Dhaka, "Report on -Soil Investigation for Proposed 20 Storied Commercial Building at 195, Motijheel Commercial Area", Dhaka.

Unique Boring & Engineering (UBE), (1995), 34 Green Road, "Nowab Mansion (3rd Floor) Dhaka, Report on -Geotechnical Investigation for Construction of Multistoried Building, Shinepukur Holdings Ltd. at Green Road", Dhaka.

Wroth, C.P. (1975), "In-situ Measurement of Initial Stresses and Deformation Characteristics", Proc. of the Specialty Conf. in In-situ Measurement of Soil Properties, ASCE, Raleigh, North Carolina, June; 181-230.

Yasin, S.J.M. (1990), "Effect of Particle Characteristics on the Strength and Volume Change Behavior of Selected Granular Deposits of Bangladesh", M.Sc. Engg. Thesis, Department of Civil Engineering, Bangladesh University of Engineering and Technology, Dhaka.

Zienkiewicz, O.C. (1977), *The Finite Element Method*, 3rd ed., McGraw-Hill Book Company, New York; 787.

TABLE 1. Soil parameters for Clay layer

	Depth (m)	Soil Type	$\kappa$	$\lambda$	$e_{cs}$	M	$\nu$	$\gamma_{bulk}$ (kN/m <sup>3</sup> )	$K_x$ (m/s)	$K_y$ (m/s)
Pile A	0-3.3	Clay above W.T.	0.01875	0.075	0.81	0.898	0.25	13.5	8E-10	5.3E-10
	3.3-8.3	Clay below W.T.	0.01875	0.075	0.81	0.898	0.25	19.0	8E-10	5.3E-10
Pile B	0.0-3.0	Clay above W.T.	0.015	0.075	0.81	0.898	0.25	13.5	8E-10	5.3E-10
	3.0-5.25	Clay below W.T.	0.015	0.075	0.81	0.898	0.25	19.0	8E-10	5.3E-10
Pile C	0-3.0	Clay above	8.75E-3	0.035	0.93	0.898	0.25	13.5	8E-10	5.3E-10
	3.0-5.5	Clay below	8.75E-3	0.035	0.93	0.898	0.25	19.0	8E-10	5.3E-10

TABLE 2. Soil parameters for Sand layer

	Depth (m)	$E_o$ (kN/m <sup>2</sup> )	$\nu$	C	$\phi$ (deg)	$Y_o$ (m)	$\gamma_{bulk}$ (kN/m <sup>3</sup> )	$K_x$ (m/s)	$K_y$ (m/s)	Rate $m_1$ (kN/m <sup>2</sup> )/m
Pile A	8.33-34.3	50E3	0.2	0	31	28.3	19.5	5E-4	3E-4	2.E3
Pile B	5.25-25.25	45.0E3	0.2	0	35	20.25	19.5	5E-4	3E-4	3.5E3
Pile C	5.5-19.25	35.0E3	0.2	0	35	14.25	19.5	5E-4	3E-4	3.5E3

TABLE 3. Interface element parameters

	Depth (m)	C (kN/m <sup>2</sup> )	$\phi$ (deg)	$K_n$ (kN/m <sup>2</sup> )	$G_s$ (kN/m <sup>2</sup> )	$G_{res}$ (kN/m <sup>2</sup> )
Pile A	0-8.33	5	23	23.34 E4	1.01 E4	10
	8.33-19.3	0	31	54.90 E4	2.1 E4	10
Pile B	0-5.25	5	23	23.34 E4	1.01 E4	10
	5.25-15.25	0	35	54.9 E4	2.1 E4	10
Pile C	0-5.5	5	23	23.34 E4	1.01 E4	10
	5.5-11	0	35	48.31 E4	1.86 E4	10

TABLE 4. Parameters for Pile Material

	E (kN/m <sup>2</sup> )	$\nu$	$\gamma_{bulk}$ (kN/m <sup>3</sup> )
Pile A	30 E6	0.20	23.5
Pile B	30 E6	0.20	23.5
Pile C	30 E6	0.20	23.5

TABLE 5. In-situ Stresses for different layers

	Depth (m)	$\sigma_v'$ (kN/m <sup>2</sup> )	$\sigma_h'$ (kN/m <sup>2</sup> )	$U_o$ (kN/m <sup>2</sup> )	$p_c'$ (kN/m <sup>2</sup> )
Pile A	0-3.3	44.55	27.143	0.0	44.35
	3.3-8.3	89.55	54.56	50.0	89.145
	8.3-34.3	336.55	163.215	310.0	0.0
Pile B	0-3.0	40.50	24.675	0.0	40.32
	3.0-5.25	60.75	37.013	22.5	60.48
	5.25-25.25	250.75	121.604	222.50	00.00
Pile C	0-3.0	40.50	24.675	0.0	40.32
	3.0-5.5	63.00	38.384	25.0	62.72
	5.5-19.25	193.63	93.900	162.50	00.00

TABLE 6. Parameters used in fixing  $C_1$

$m_r$ (m/element)	$C_1$ (m)	$C_2$ (m)	$L_1$	$N_1$	$N_2$	$T_1$ (m)
1.0,0.5,0.25 0.125	20	15	$L_1$	20	2	0.05

TABLE 7. Parameters used in analysis for  $N_2$

$m_r$ (m/element)	$C_1$ (m)	$C_2$ (m)	$L_1$	$N_1$	$N_2$	$T_1$ (m)
0.5	20	15	$L_1$	20	2,3,4	0.05

TABLE 8. Final parameters of mesh configuration

$m_r$ (m/cl.)	$C_1$ (m)	$C_2$ (m)	$L_1$	$N_1$	$N_2$	$T_1$ (m)
D	H	0.75H	$L_1$	$H/(2D)$	4 (D/2)	(1/10) (D/2)